

# Non-Hermitian planar elastic metasurface for unidirectional focusing of flexural waves

Cite as: Appl. Phys. Lett. **120**, 241701 (2022); doi: [10.1063/5.0097177](https://doi.org/10.1063/5.0097177)

Submitted: 26 April 2022 · Accepted: 4 June 2022 ·

Published Online: 13 June 2022




View Online



Export Citation



CrossMark

Katerina Stojanoska and Chen Shen<sup>a)</sup> 

## AFFILIATIONS

Department of Mechanical Engineering, Rowan University, Glassboro, New Jersey 08028, USA

Note: This paper is part of the APL Special Collection on Acoustic and Elastic Metamaterials and Metasurfaces.

<sup>a)</sup> Author to whom correspondence should be addressed: [shenc@rowan.edu](mailto:shenc@rowan.edu)

## ABSTRACT

Metasurfaces exhibiting spatially asymmetric inner structures have been shown to host unidirectional scattering effects, benefiting areas where directional control of waves is desired. In this work, we propose a non-Hermitian planar elastic metasurface to achieve unidirectional focusing of flexural waves. The unit cells are constructed by piezoelectric disks and metallic blocks that are asymmetrically loaded. A tunable material loss is then introduced by negative capacitance shunting. By suitably engineering the induced loss profile, a series of unit cells are designed, which can individually access the exceptional points manifested by unidirectional zero reflection. We then construct a planar metasurface by tuning the reflected phase to ensure constructive interference at one side of the metasurface. Unidirectional focusing of the incident waves is demonstrated, where the reflected wave energy is focused from one direction, and zero reflection is observed in the other direction. The proposed metasurface enriches the flexibility in asymmetric elastic wave manipulation as the loss and the reflected phase can be tailored independently in each unit cell.

Published under an exclusive license by AIP Publishing. <https://doi.org/10.1063/5.0097177>

The notion of parity-time (PT) symmetry was first proposed by Bender and Boettcher in 1998,<sup>1</sup> where it is found that the behavior of PT-symmetric systems can change dramatically at a state transition from real to complex energies. At this point, the symmetry of the system would be broken, and real spectra in the Hamiltonian are achieved. A necessary condition for PT-symmetry is that for the Hamiltonian potential, it must be even in its real part and odd in its imaginary part. Once the imaginary part reaches a certain threshold, a break in PT symmetry can be observed, which causes an abrupt change in the real energy spectrum.<sup>2–4</sup> This transition corresponds to an exceptional point (EP) where the eigenstates become degenerate. Thanks to the mathematical equivalence between the Schrödinger's equation and the paraxial electromagnetic wave equations,<sup>2,5</sup> the study of EP has been extended to a plethora of physical systems other than quantum mechanics. Such systems comprise acoustics,<sup>6–11</sup> optics,<sup>12–19</sup> photonics,<sup>20–25</sup> among many others.

Recently, in the field of acoustics and elastodynamics, it is found that the occurrence of EP could be related to Willis coupling<sup>26–28</sup> where a cross coupling between stress and velocity or momentum and strain exists. To achieve this phenomenon, the eigenstates of the scattering matrix must coalesce. Due to the fascinating effects the Willis coupling possesses, there has been an upsurge of interest in this area in

recent years.<sup>29–32</sup> For example, perfect wavefront transformation with 100% conversion efficiency has been proposed based on the concept where the input energy is directed to the intended direction without diffraction or scattering into undesirable directions.<sup>33–35</sup> In the field of elastic waves, such a coupling effect has also been found in nondestructive testing and structural-health monitoring.<sup>36,37</sup> Willis coupling typically takes place when the structures are geometrically asymmetric. It is found that when loss is added to the system and a non-Hermitian description is needed, EPs can be engineered by carefully tailoring the loss and the structure asymmetry, such that unidirectional zero reflection is achieved.<sup>26</sup> Recent studies have shown that Willis material can be used for manipulating flexural waves using artificial structures<sup>28</sup> as well as for constructing unidirectional reflectionless acoustic devices<sup>27</sup> to achieve purposeful sound insulation and steering. However, existing metasurfaces that host EPs either do not have planar geometry or are difficult to individually control the loss profile in their unit cells, limiting their practical usage in different scenarios.

In this paper, we are extending the concept by proposing a planar non-Hermitian elastic metasurface for the control of flexural waves. With the loss being induced by negative capacitance piezoelectric shunting, symmetry breaking takes place followed by an emergence of EPs. The numerical simulations show strong asymmetric reflection

properties, i.e., zero reflection in the immediate vicinity of the EPs when the structure is ensouffled from one side. Additionally, with the waves being incident on the other side, there is an occurrence of focusing of the waves. Thus, a desired asymmetric control of flexural waves can be achieved with the planar elastic metasurface. The loss can be conveniently tuned by varying the negative capacitance shunting of the piezoelectric disks, thus enabling other potential applications.

We consider flexural wave propagation on a thin elastic beam made of acrylic. The geometry of the building block is shown in Fig. 1(a), where a cavity is perforated on the beam, and a piezoelectric disk and a metallic block are connected in series. In this way, the unit cell is loaded asymmetrically since the piezoelectric disk is only attached to one side of the cavity. As shown in previous works,<sup>26,28</sup> this spatial asymmetry can lead to different scattering properties for waves incident from opposite directions. To achieve a larger degree of asymmetry, each unit cell of the metasurface is composed of five individual building blocks, as illustrated in Fig. 1(b). We define the forward direction when the piezoelectric disk is placed in front of the metallic block. Here, the piezoelectric material is chosen as Lead Zirconate Titanate (PZT-5H) with dimensions being  $l_p = 1$  mm,  $w_p = 3$  mm, and  $h_p = 0.585$  mm. The metallic block is made of lead with  $l_l = 1.5$  mm,  $w_l = 3$  mm, and  $h_l = 3.9$  mm, and the size of the acrylic beam building

block is  $l_a = 5$  mm,  $w_a = 6$  mm, and  $h_a = 2$  mm. The total length of the unit cell of the metasurface is, therefore, 25 mm.

To this end, numerical simulations based on finite element analysis are performed to study the scattering properties of the metasurface unit cell using COMSOL Multiphysics. The material properties used in the simulations are density of 1190 and 11 340 kg/m<sup>3</sup>, Young's modulus of 3.20 and 16 GPa, and Poisson's ratio of 0.29 and 0.44, respectively, for acrylic beam and lead. It should be noted that no loss is introduced at the moment for PZT-5H, and it has a density, short circuit modulus, Poisson's ratio, and electromechanical coupling coefficient of 7500 kg/m<sup>3</sup>, 60.6 GPa, 0.34, and 0.36, respectively. Out-of-plane flexural waves are excited from one end of the unit cell within the frequency range between 5000 and 7500 Hz.

The amplitude and the phase of the reflection and transmission coefficients are shown in Figs. 1(c) and 1(d), respectively. It is expected that the amplitude of the reflected and transmitted wave should be the same regardless of the propagation direction of the waves as the structure is entirely passive and lossless. The slight difference is likely caused by the numerical errors in the simulations. The reflected phase, on the contrary, is different depending on the incident wave direction, which is a result of the structural asymmetry of the unit cells.

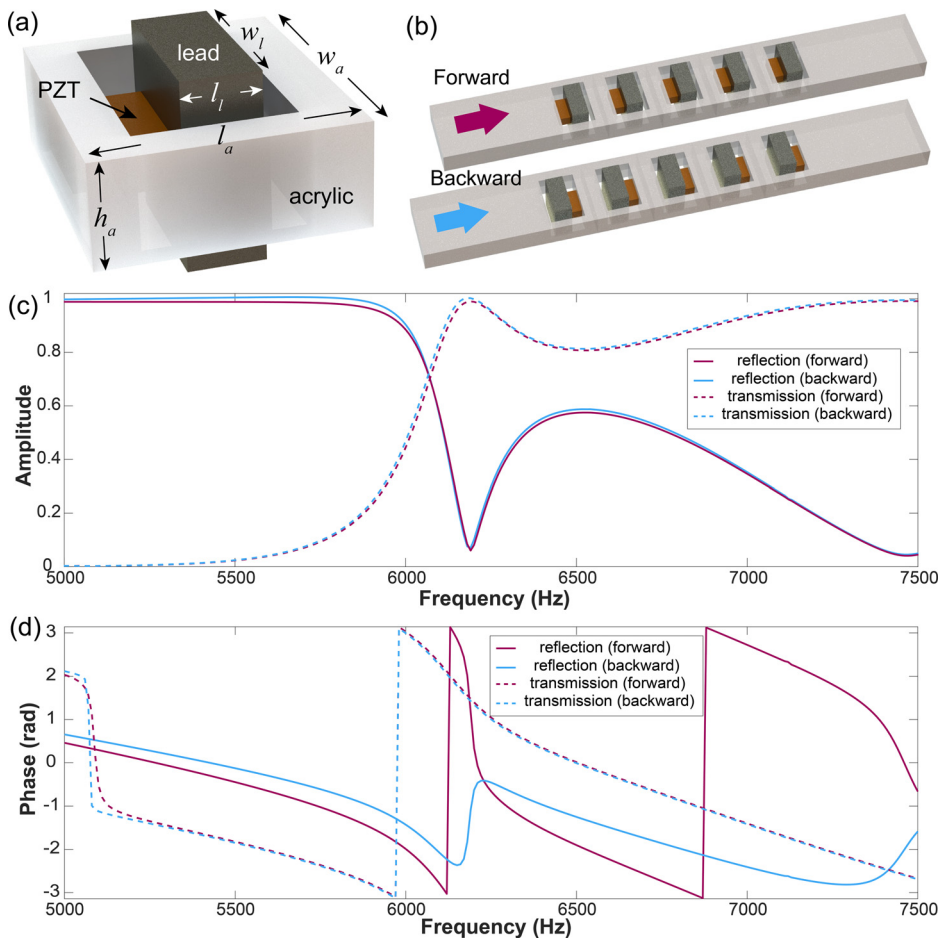


**FIG. 1.** (a) Schematic view of the one resonating building block. (b) Forward and backward views of the unit cell with given directions of the flexural waves. (c) Amplitude of the reflection and transmission coefficients for the flexural wave propagating in forward and backward directions. (d) Phase shift of the reflection and transmission coefficients for the flexural wave propagating in forward and backward directions.

To further break the symmetry of the system, loss is added to the structures. The introduction of loss will make the system non-Hermitian as manifested by the change of the reflection amplitudes. Here, the loss is induced by a shunted circuit connected to the piezoelectric disk.<sup>36,38</sup> The effective Young's modulus, including the loss factor, can be modified by applying the negative capacitance shunting circuit, which is shown in Fig. 2(a). The equivalent capacitance  $C_n$  realized by the circuit can be tuned by the  $R_1$ ,  $R_2$ , and  $C$  values, and the modified effective Young's modulus is expressed as<sup>38</sup>

$$E_p = E_p^E \frac{C_p^T - C_n}{C_p^T(1 - k_{31}^2) - C_n}, \quad (1)$$

where  $C_p^T$ ,  $C_n$ ,  $E_p^E$ , and  $k_{31}$  represent the capacitance of the piezoelectric disk, the capacitance of the circuit, the short circuit modulus, and the electromechanical coupling coefficient, respectively.

The loss can, thus, be conveniently tuned by the shunting resistance and the negative capacitance. Compared to other approaches such as attaching a soft porous rubber to the beam,<sup>28</sup> it provides an easy means to tune the loss of the PZT. This will greatly facilitate the design of the unit cells as well as the metasurface since the loss profile needs to be carefully adjusted, as will be shown later. It is important to point out that the intrinsic loss of the host beam is not considered in the simulation. If necessary, the induced loss by negative capacitance shunting can be adjusted, such that the overall loss leads to zero reflection from the forward direction.

As shown in Fig. 2(b), at the resonance frequency of 6190 Hz, the reflection amplitude of the wave propagating in the forward direction is finite when the system is lossless. The amplitude changes as we increase the loss factor monotonically. Remarkably, when a loss factor of 0.02 is introduced, the unit cell exhibits unidirectional zero reflection, i.e., the reflection amplitude approaches zero in the forward direction, while it is finite in the backward direction. Furthermore, when the loss factor passes this critical value, the amplitude is changed and is no longer zero. In addition, when we are taking

into consideration the propagating wave being incident from a backward direction as illustrated in Fig. 2(c), it is obvious that the amplitude is the same as the amplitude of the wave propagating in a forward direction when the system is assumed lossless. To additionally elaborate, an introduction of a particular loss at the same frequency of 6190 Hz clearly shows that the reflection amplitudes for the propagating wave in the backward direction differ from the forward, representing an asymmetry; thus, the reflection never reaches zero. At this point, it is obvious as expected that the scattering matrix no longer remains unitary. It is important to point out that the transmission amplitudes of the propagating wave stay the same regardless of the amount of the added loss because the system is reciprocal albeit it is lossy. To further confirm the behavior at this frequency and its relation to EP, the eigenvalues of the scattering matrix are calculated as a function of the induced loss factor at 6190 Hz, and the results are presented in Fig. 3. It can be seen that when the loss factor is tuned to 0.02, there is a coalescence of the real and the imaginary parts of the eigenvalues. A biased distribution is observed before and after the occurrence of the EP in Figs. 3(a) and 3(b), respectively, for the real and the imaginary parts. The absolute values also undergo a phase transition at this point. As such, the two eigenstates become degenerate as shown in Fig. 3(c). This peculiar behavior is a clear sign of the emergence of EP in the system.

A metasurface is further designed to achieve a unidirectional focusing effect. This is achieved by designing a series of unit cells that all host EP in the forward direction but have different reflected phases in the backward direction. From previous simulations, we have confirmed that the wavelength of the flexural wave is  $\lambda = 30.66$  mm at 6190 Hz, and the width of the unit cells, on the contrary, is  $w_a = 6$  mm, which is about 1/5 of the wavelength. This helps to achieve enough spatial resolution of the metasurface. The focal distance is assumed to be  $d = 60$  mm, and the required phase of the metasurface is calculated by the constructive interference at the focal point,

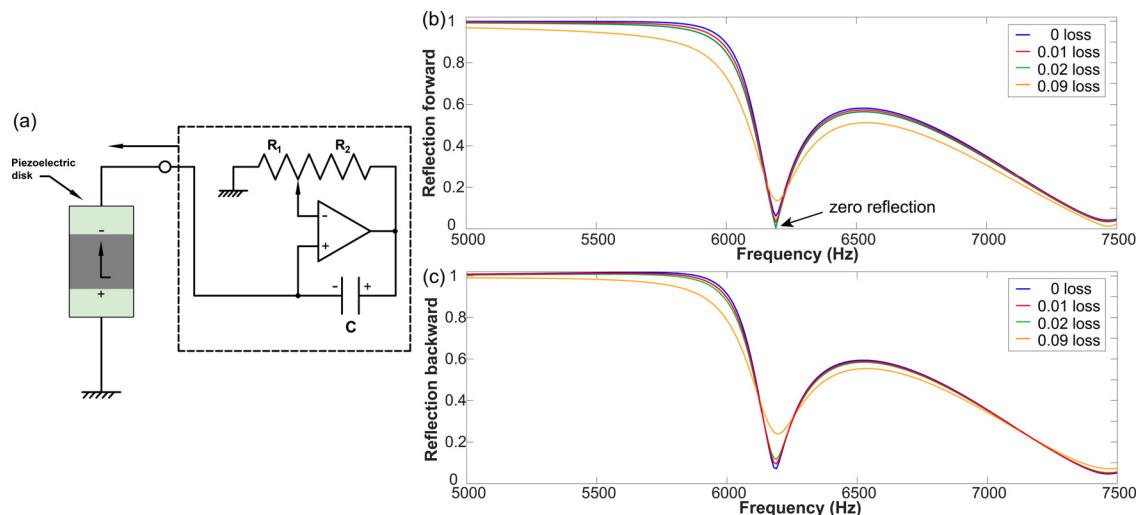


**FIG. 2.** (a) Piezoelectric disk connected to a negative capacitance shunting circuit. (b) Amplitude of the reflection coefficient for the flexural wave propagating in a forward direction for different loss patterns. (c) Amplitude of the reflection coefficient for the flexural wave propagating in a backward direction for different loss patterns.

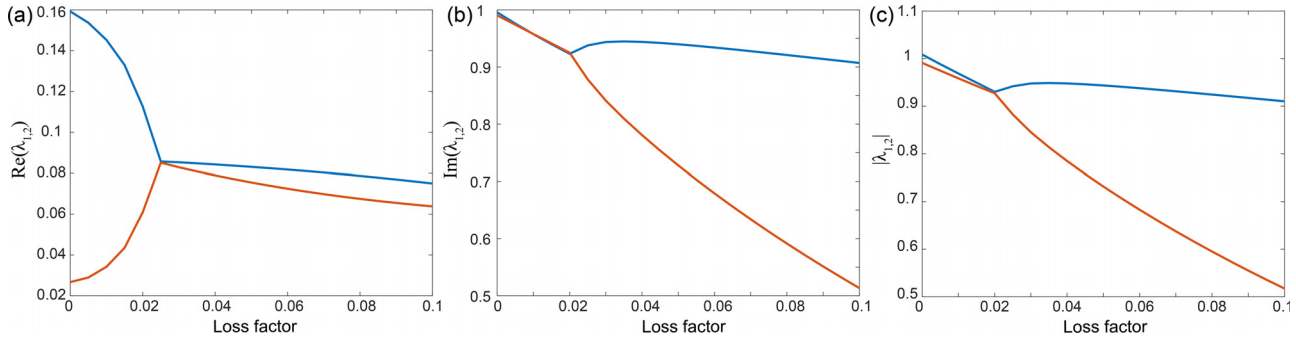


FIG. 3. Real (a), imaginary (b), and absolute values (c) of the eigenvalues of the S matrix at 6190 Hz.

$$\phi = 2\pi \frac{\sqrt{d^2 + \Delta x^2} - d}{\lambda}, \quad (2)$$

where  $\Delta x$  is the lateral distance from the center of the metasurface. The required phase is illustrated by the blue curve in Fig. 4, while the red circles mark the actual phase of the designed unit cells. A total number of eight unit cells are designed, which cover a phase shift of around  $\pi$ . The geometry of each unit cell is obtained by tuning the height of the metallic blocks as well as the piezoelectric disks while keeping the unidirectional zero reflection behavior. The corresponding dimensions and the associated loss factors for each unit cell are given in Table I. It should be noted that the loss factors are different for each individual unit cell in order to achieve EP. In other words, the loss profile of the entire metasurface needs to be carefully modulated, such that all the unit cells can access their respective EP. The negative capacitance shunting mechanism provides a convenient means to adjust the loss in each unit without physically altering the structure or adding additional materials. The designed metasurface consists of 16 resonator-based unit cells, placed symmetrically about the center of the metasurface, in order to achieve a unidirectional focusing effect.

Figure 5(a) shows that when the flexural wave is excited in the forward direction at 6190 Hz, the wavefront remains planar, and very

little interference is observed on the reflection side, which indicates zero reflection is achieved. This is because each unit cell is tailored to exhibit EP at the operation frequency; hence, net-zero reflection is achieved for the entire metasurface. On the contrary, the interference pattern is vastly different for flexural waves propagating from the opposite direction. Different local reflection coefficients are induced at the unit cells, and focusing of reflected waves is achieved based on constructive interference at the far-field. Such phenomenon is confirmed by Fig. 5(b), which displays a focusing pattern. The focal point is around 55 mm away from the metasurface, which is slightly different from the designed value as  $d = 60$  mm. This can be explained by the non-ideal reflected phase and the coupling and interactions among the unit cells. Nevertheless, the metasurface exhibits strong asymmetric scattering properties that could be of great importance where directional wave manipulation is desired. As for the difference on the transmission side, it is likely caused by the diffractions at the metasurface since its width is much larger than the corresponding wavelength. This is similar to the case where a wide waveguide that supports multiple modes can lead to different transmission patterns for incident wave from different directions.<sup>39</sup> It should be noted that, however, such an asymmetry does not break the reciprocity of the system. Moreover, to quantitatively evaluate the focusing effect by the metasurface, the displacement amplitude of the reflected waves is extracted at a distance of  $d = 55$  mm away from the metasurface. The result is shown in Fig. 5(c), and a clear focal profile is observed. The full width at half maximum (FWHM) is around  $0.83\lambda$ . The focusing effect may

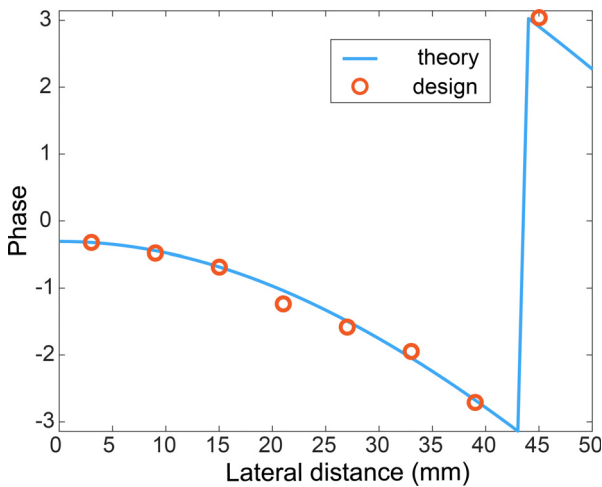
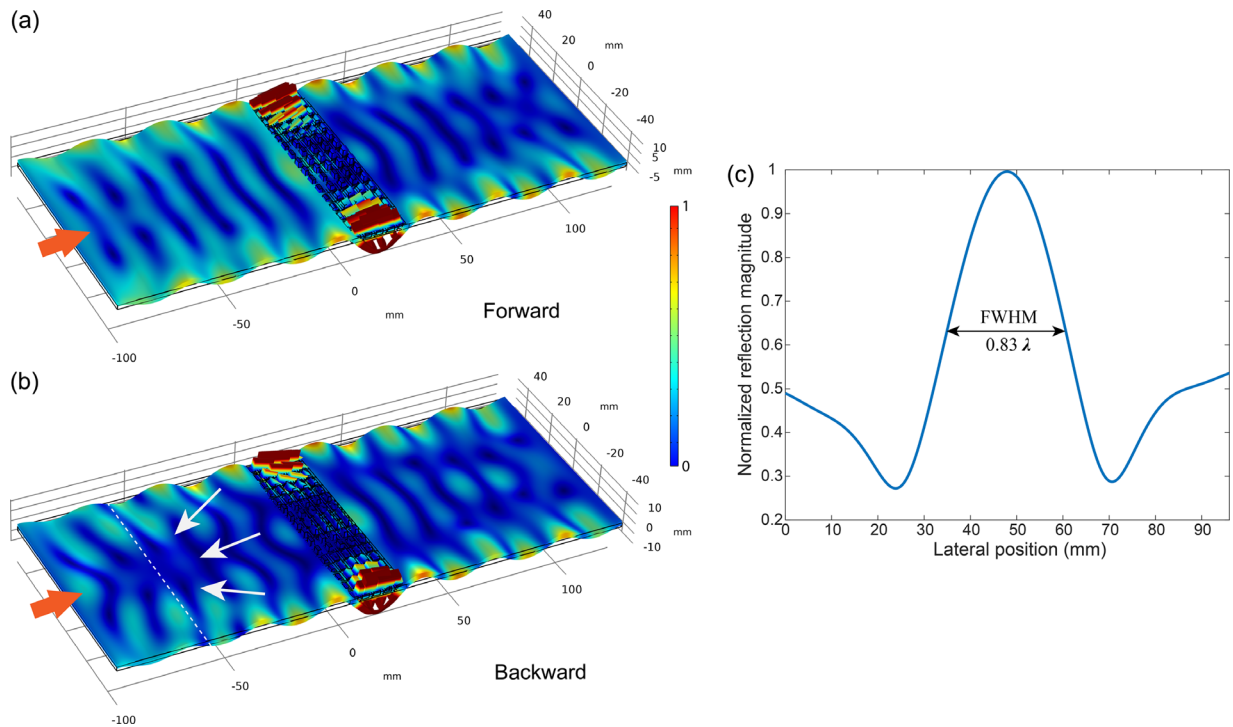


FIG. 4. Theoretically calculated vs designed phase for achieving a unidirectional focusing effect.

TABLE I. Corresponding dimensions and loss factors for each unit cell.

Unit cell number	Height of lead (mm)	Height of PZT (mm)	Loss factor
1	6.5	1.56	0.05
2	6.0	1.21	0.04
3	5.5	1.01	0.04
4	3.9	0.59	0.02
5	3.5	0.51	0.02
6	2.8	0.41	0.02
7	2.2	0.34	0.02
8	2.0	0.32	0.01





**FIG. 5.** (a) Displacement magnitude of the metasurface with incident waves in the forward direction. (b) Displacement magnitude of the metasurface with incident waves in the backward direction. (c) Normalized reflection magnitude from the cutline at  $d = 55$  mm.

be further increased by improving the design, e.g., with more unit cells that cover a larger phase shift.

To conclude, we have proposed a non-Hermitian planar elastic metasurface for a unidirectional focusing effect using Willis materials. The metasurface contains piezoelectric materials and metallic blocks that are asymmetrically loaded, and the loss is introduced by the shunted piezos. The proposed design works for flexural waves on elastic structures. Unidirectional zero reflection is achieved when approaching the EP of the scattering matrix in the unit cells by tuning the losses, which are represented as a non-Hermitian system. Furthermore, a unidirectional focusing effect is achieved based on a metasurface composed of a series of unit cells. The backward propagation of the waves shows that there is a focus of the wave energy due to the constructed phase of the reflection waves, while negligible reflection is observed from the other side. Compared to curved metasurfaces that achieve similar effects,<sup>40</sup> the compact and planar structure is easy to be integrated into existing structures and can be applied in various scenarios. The ability to tune the unit cells individually offers a greater design degree of freedom by controlling the reflections from different directions. For example, other unidirectional wave devices can be synthesized by engineering the reflected phase based on the same concept to achieve other types of beam engineering, e.g., beam steering, accelerating beams, and so on. The proposed mechanism can be also used in different types of elastic waves, such as bulk and surface waves by the means of a suitable design and introduction of loss. As of experimental implementation, a potential challenge is the complexity of the metasurface due to the individual tuning of the unit cells and external circuits.<sup>41</sup> It is hoped

that the proposed system will bring about additional possibilities for elastic wave manipulation for applications in structural health monitoring and nondestructive testing. Further improvement of the design may be done by optimization of the unit cells to be able to cover a full phase shift of  $2\pi$  to achieve other functionalities.

This material was based on work supported by the National Science Foundation under Grant No. 2137749.

## AUTHOR DECLARATIONS

### Conflict of Interest

The authors have no conflicts to disclose.

### Author Contributions

**Katerina Stojanoska:** Data curation (equal); Formal analysis (equal); Writing – original draft (equal). **Chen Shen:** Conceptualization (equal); Formal analysis (equal); Funding acquisition (equal); Project administration (equal); Writing – review and editing (equal).

### DATA AVAILABILITY

The data that support the findings of this study are available from the corresponding author upon reasonable request.

### REFERENCES

- <sup>1</sup>C. M. Bender and S. Boettcher, “Real spectra in non-Hermitian Hamiltonians having  $\mathcal{PT}$  symmetry,” *Phys. Rev. Lett.* **80**, 5243 (1998).
- <sup>2</sup>C. M. Bender, “Making sense of non-Hermitian Hamiltonians,” *Rep. Prog. Phys.* **70**, 947 (2007).

- <sup>3</sup>L. Feng, R. El-Ganainy, and L. Ge, “Non-Hermitian photonics based on parity-time symmetry,” *Nat. Photonics* **11**, 752–762 (2017).
- <sup>4</sup>R. El-Ganainy, K. G. Makris, M. Khajavikhan, Z. H. Musslimani, S. Rotter, and D. N. Christodoulides, “Non-Hermitian physics and PT symmetry,” *Nat. Phys.* **14**, 11–19 (2018).
- <sup>5</sup>C. M. Bender, D. C. Brody, and H. F. Jones, “Complex extension of quantum mechanics,” *Phys. Rev. Lett.* **89**, 270401 (2002).
- <sup>6</sup>X. Zhu, H. Ramezani, C. Shi, J. Zhu, and X. Zhang, “ $\mathcal{PT}$ -symmetric acoustics,” *Phys. Rev. X* **4**, 031042 (2014).
- <sup>7</sup>R. Fleury, D. Sounas, and A. Alu, “An invisible acoustic sensor based on parity-time symmetry,” *Nat. Commun.* **6**, 1–7 (2015).
- <sup>8</sup>C. Shi, M. Dubois, Y. Chen, L. Cheng, H. Ramezani, Y. Wang, and X. Zhang, “Accessing the exceptional points of parity-time symmetric acoustics,” *Nat. Commun.* **7**, 1–5 (2016).
- <sup>9</sup>J. Christensen, M. Willatzen, V. Velasco, and M.-H. Lu, “Parity-time synthetic phononic media,” *Phys. Rev. Lett.* **116**, 207601 (2016).
- <sup>10</sup>V. Achilleos, G. Theoharis, O. Richoux, and V. Pagneux, “Non-Hermitian acoustic metamaterials: Role of exceptional points in sound absorption,” *Phys. Rev. B* **95**, 144303 (2017).
- <sup>11</sup>Y. Zhou, Z.-Z. Yang, Y.-Y. Peng, and X.-Y. Zou, “Parity-time-symmetric acoustic system constructed by piezoelectric composite plates with active external circuits,” *Chin. Phys. B* **31**, 064304 (2022).
- <sup>12</sup>A. Guo, G. Salamo, D. Duchesne, R. Morandotti, M. Volatier-Ravat, V. Aimez, G. Siviloglou, and D. Christodoulides, “Observation of  $\mathcal{PT}$ -symmetry breaking in complex optical potentials,” *Phys. Rev. Lett.* **103**, 093902 (2009).
- <sup>13</sup>C. E. Rüter, K. G. Makris, R. El-Ganainy, D. N. Christodoulides, M. Segev, and D. Kip, “Observation of parity-time symmetry in optics,” *Nat. Phys.* **6**, 192–195 (2010).
- <sup>14</sup>Z. Lin, H. Ramezani, T. Eichelkraut, T. Kottos, H. Cao, and D. N. Christodoulides, “Unidirectional invisibility induced by  $\mathcal{PT}$ -symmetric periodic structures,” *Phys. Rev. Lett.* **106**, 213901 (2011).
- <sup>15</sup>L. Feng, Y.-L. Xu, W. S. Fegadolli, M.-H. Lu, J. E. Oliveira, V. R. Almeida, Y.-F. Chen, and A. Scherer, “Experimental demonstration of a unidirectional reflectionless parity-time metamaterial at optical frequencies,” *Nat. Mater.* **12**, 108–113 (2013).
- <sup>16</sup>J. Wen, X. Jiang, L. Jiang, and M. Xiao, “Parity-time symmetry in optical micro-cavity systems,” *J. Phys. B* **51**, 222001 (2018).
- <sup>17</sup>M. Moccia, G. Castaldi, F. Monticone, and V. Galdi, “Exceptional points in flat optics: A non-Hermitian line-wave scenario,” *Phys. Rev. Appl.* **15**, 064067 (2021).
- <sup>18</sup>J. Xie, S. Dong, B. Yan, Y. Peng, C. Qiu, S. Wen *et al.*, “Simple theoretical model for parity-time-symmetric metasurfaces,” [arXiv:2107.10506](https://arxiv.org/abs/2107.10506) (2021).
- <sup>19</sup>L. Wang, F. Liu, F. Liu, Z. Qin, Y. Zhang, D. Zhong, and H. Ni, “Optical fractal and exceptional points in PT symmetry Thue-Morse photonic multilayers,” *Opt. Mater.* **123**, 111821 (2022).
- <sup>20</sup>A. Regensburger, C. Bersch, M.-A. Miri, G. Onishchukov, D. N. Christodoulides, and U. Peschel, “Parity-time synthetic photonic lattices,” *Nature* **488**, 167–171 (2012).
- <sup>21</sup>Y. Lumer, Y. Plotnik, M. C. Rechtsman, and M. Segev, “Nonlinearly induced  $\mathcal{PT}$  transition in photonic systems,” *Phys. Rev. Lett.* **111**, 263901 (2013).
- <sup>22</sup>B. Peng, Ş. K. Özdemir, F. Lei, F. Monifi, M. Gianfreda, G. L. Long, S. Fan, F. Nori, C. M. Bender, and L. Yang, “Parity-time-symmetric whispering-gallery microcavities,” *Nat. Phys.* **10**, 394–398 (2014).
- <sup>23</sup>M. Lawrence, N. Xu, X. Zhang, L. Cong, J. Han, W. Zhang, and S. Zhang, “Manifestation of  $\mathcal{PT}$  symmetry breaking in polarization space with terahertz metasurfaces,” *Phys. Rev. Lett.* **113**, 093901 (2014).
- <sup>24</sup>M. Wu, F. Liu, D. Zhao, and Y. Wang, “Unidirectional invisibility in  $\mathcal{PT}$ -symmetric cantor photonic crystals,” *Crystals* **12**, 199 (2022).
- <sup>25</sup>N. Maraviglia, P. Yard, R. Wakefield, J. Carolan, C. Sparrow, L. Chakhmakhchyan, C. Harrold, T. Hashimoto, N. Matsuda, A. K. Harter *et al.*, “Photonic quantum simulations of coupled  $\mathcal{PT}$ -symmetric Hamiltonians,” *Phys. Rev. Res.* **4**, 013051 (2022).
- <sup>26</sup>C. Shen, J. Li, X. Peng, and S. A. Cummer, “Synthetic exceptional points and unidirectional zero reflection in non-Hermitian acoustic systems,” *Phys. Rev. Mater.* **2**, 125203 (2018).
- <sup>27</sup>A. Merkel, V. Romero-García, J.-P. Groby, J. Li, and J. Christensen, “Unidirectional zero sonic reflection in passive  $\mathcal{PT}$ -symmetric Willis media,” *Phys. Rev. B* **98**, 201102 (2018).
- <sup>28</sup>Y. Liu, Z. Liang, J. Zhu, L. Xia, O. Mondain-Monval, T. Brunet, A. Alù, and J. Li, “Willis metamaterial on a structured beam,” *Phys. Rev. X* **9**, 011040 (2019).
- <sup>29</sup>S. Koo, C. Cho, J.-H. Jeong, and N. Park, “Acoustic omni meta-atom for decoupled access to all octants of a wave parameter space,” *Nat. Commun.* **7**, 1–7 (2016).
- <sup>30</sup>M. B. Muhlestein, C. F. Sieck, P. S. Wilson, and M. R. Haberman, “Experimental evidence of Willis coupling in a one-dimensional effective material element,” *Nat. Commun.* **8**, 1–9 (2017).
- <sup>31</sup>C. F. Sieck, A. Alù, and M. R. Haberman, “Origins of Willis coupling and acoustic bianisotropy in acoustic metamaterials through source-driven homogenization,” *Phys. Rev. B* **96**, 104303 (2017).
- <sup>32</sup>X. Su and A. N. Norris, “Retrieval method for the bianisotropic polarizability tensor of Willis acoustic scatterers,” *Phys. Rev. B* **98**, 174305 (2018).
- <sup>33</sup>A. Díaz-Rubio and S. A. Tretyakov, “Acoustic metasurfaces for scattering-free anomalous reflection and refraction,” *Phys. Rev. B* **96**, 125409 (2017).
- <sup>34</sup>J. Li, C. Shen, A. Díaz-Rubio, S. A. Tretyakov, and S. A. Cummer, “Systematic design and experimental demonstration of bianisotropic metasurfaces for scattering-free manipulation of acoustic wavefronts,” *Nat. Commun.* **9**, 1–9 (2018).
- <sup>35</sup>L. Quan, Y. Ra’di, D. L. Sounas, and A. Alù, “Maximum Willis coupling in acoustic scatterers,” *Phys. Rev. Lett.* **120**, 254301 (2018).
- <sup>36</sup>Z. Chen, M. Negahban, Z. Li, and J. Zhu, “Tunable exceptional point and unidirectional zero reflection of a metabeam using shunted piezos,” *J. Phys. D* **53**, 095503 (2020).
- <sup>37</sup>X. Li, Z. Yu, H. Iizuka, and T. Lee, “Experimental demonstration of extremely asymmetric flexural wave absorption at the exceptional point,” *Extreme Mech. Lett.* **52**, 101649 (2022).
- <sup>38</sup>Y. Chen, G. Huang, and C. Sun, “Band gap control in an active elastic metamaterial with negative capacitance piezoelectric shunting,” *J. Vib. Acoust.* **136**, 061008 (2014).
- <sup>39</sup>J. Zhu, X. Zhu, X. Yin, Y. Wang, and X. Zhang, “Unidirectional extraordinary sound transmission with mode-selective resonant materials,” *Phys. Rev. Appl.* **13**, 041001 (2020).
- <sup>40</sup>T. Liu, X. Zhu, F. Chen, S. Liang, and J. Zhu, “Unidirectional wave vector manipulation in two-dimensional space with an all passive acoustic parity-time-symmetric metamaterials crystal,” *Phys. Rev. Lett.* **120**, 124502 (2018).
- <sup>41</sup>X. Li, Y. Chen, R. Zhu, and G. Huang, “An active meta-layer for optimal flexural wave absorption and cloaking,” *Mech. Syst. Signal Process.* **149**, 107324 (2021).